Title
Lipin-1 and lipin-3 together determine adiposity in vivo

Journal
Molecular Metabolism, 3(2)

ISSN
2212-8778

Authors
Csaki, Lauren S
Dwyer, Jennifer R
Li, Xia
et al.

Publication Date
2014-04-01

DOI
10.1016/j.molmet.2013.11.008

Peer reviewed

Original article

MOLECULAR METABOLISM

Lipin-1 and lipin-3 together determine adiposity *in vivo*⋆

Lauren S. Csaki [1], Jennifer R. Dwyer [2], Xia Li [1], Michael H.K. Nguyen [1], Jay Dewald [3], David N. Brindley [3], Aldons J. Lusis [1,4,5], Yuko Yoshinaga [6,7], Pieter de Jong [6], Loren Fong [4], Stephen G. Young [1,2,4], Karen Reue [1,2,4,⋆]

ABSTRACT

The lipin protein family of phosphatidate phosphatases has an established role in triacylglycerol synthesis and storage. Physiological roles for lipin-1 and lipin-2 have been identified, but the role of lipin-3 has remained mysterious. Using lipin single- and double-knockout models we identified a cooperative relationship between lipin-3 and lipin-1 that influences adipogenesis *in vitro* and adiposity *in vivo*. Furthermore, natural genetic variations in *Lpin1* and *Lpin3* expression levels across 100 mouse strains correlate with adiposity. Analysis of PAP activity in additional metabolic tissues from lipin single- and double-knockout mice also revealed roles for lipin-1 and lipin-3 in spleen, kidney, and liver, for lipin-1 alone in heart and skeletal muscle, and for lipin-1 and lipin-2 in lung and brain. Our findings establish that lipin-1 and lipin-3 cooperate *in vivo* to determine adipose tissue PAP activity and adiposity, and may have implications in understanding the protection of lipin-1-deficient humans from overt lipodystrophy.

Keywords Gene family; Knockout mouse; Adipogenesis; Triacylglycerol; Glycerolipid biosynthesis

1. INTRODUCTION

Lipins are phosphatidate phosphatase (PAP) enzymes that catalyze the penultimate step in triacylglycerol (TAG) biosynthesis, the dephosphorylation of phosphatidate to diacylglycerol [1–5]. Lipins also possess a transcriptional coactivator motif and have been shown to co-regulate the expression of fatty acid oxidation and inflammatory genes [6–10]. While invertebrates and single-celled eukaryotes possess a single lipin, mammals have three lipin family members (lipin-1, lipin-2, and lipin-3), which presumably arose through gene duplication. Mammals possess many such gene families, and in the case of enzyme families, different family members often display the capacity to carry out the same enzymatic step. The existence of multiple enzymes for the same biochemical reaction often raises questions about the precise role of each family member *in vivo*. We hypothesized that each lipin protein plays a unique physiological role despite similar enzymatic capabilities *in vitro*.

To date, most studies of mammalian lipin protein function have focused on lipin-1, the founding member of the family (reviewed in [5,10]). In the mouse, lipin-1 deficiency causes severe lipodystrophy with reduced TAG stores in adipocytes, insulin resistance [1,11,12], impaired hepatic lipid homeostasis during the neonatal period, and peripheral neuropathy in adults [13–15]. Lipin-1 is critical for PAP activity in adipose tissue, providing a ready explanation for the reduced TAG stores in the adipose tissue of lipin-1-deficient mice. Lipin-1 deficiency also lowers PAP activity in skeletal and cardiac muscle [3,4,16]. On the other hand, increased lipin-1 expression in adipose tissue increases adiposity [17,18]. In humans, lipin-1 deficiency does not cause lipodystrophy but leads to recurrent rhabdomyolysis [19–21]. The fact that humans with lipin-1 deficiency do not manifest lipodystrophy suggests that a compensatory mechanism for TAG synthesis could exist in human adipose tissue, presumably due to the activity of other lipin family members. Compensation by other lipin family members might also exist in mice. While lipin-1-deficient mice manifest overt lipodystrophy, they still have a small amount of TAG-containing adipose tissue. The existence of that small amount of adipose tissue, despite an absence of lipin-1, could be due to compensation by lipin-2 or lipin-3.

Lipin-2 and lipin-3 exhibit tissue expression patterns distinct from lipin-1 and from each other, and many tissues express multiple lipin family members. Lipin-2 is highly expressed in liver and cerebellum, but lipin-1 is also present in these tissues [7,22]. We have already shown that lipin-1 and lipin-2 are both required for adequate PAP activity under physiological stresses such as aging (in cerebellum) and high-fat feeding (in liver); however, we did not find a significant role for

[1]Department of Human Genetics, David Geffen School of Medicine at UCLA, Los Angeles, CA 90095, USA [2]Molecular Biology Institute, University of California, Los Angeles, CA 90095, USA [3]Signal Transduction Research Group, Department of Biochemistry, University of Alberta, Alberta, Canada [4]Department of Medicine, David Geffen School of Medicine at UCLA, Los Angeles, CA 90095, USA [5]Department of Microbiology, Immunology, and Molecular Genetics, David Geffen School of Medicine at UCLA, Los Angeles, CA 90095, USA [6]Children's Hospital Oakland Research Institute, Oakland, CA 94609, USA

[7]Current address: Department of Energy (DOE) Joint Genome Institute, Walnut Creek, CA 94598, USA.

*Corresponding author at: Department of Human Genetics, Gonda 6506A, 695 Charles E. Young Drive South, Los Angeles, CA 90095, United States. Tel.: +1 310 794 5631; fax: +1 310 794 5446. Email: reuek@ucla.edu (K. Reue).

Received October 30, 2013 • Revision received November 17, 2013 • Accepted November 21, 2013 • Available online 28 November 2013

http://dx.doi.org/10.1016/j.molmet.2013.11.008

lipin-2 in adipose tissue [22]. Lipin-3 is expressed in adipose tissue, as well as in kidney, intestine, heart, and liver [4,16]. Each of those tissues also expresses lipin-1 and/or lipin-2, making it difficult to define the physiological role of lipin-3. Here, we employed single- and double-knockout models to investigate the possibility that lipin-3 plays an important role in adipose tissue *in vivo*.

2. MATERIALS AND METHODS

2.1. Animal studies

*Lpin3*KO mice were generated by targeted trapping [23]. The trapping vector, which contained a splice acceptor site upstream of a promoterless β-geo cassette, was inserted into intron 3 of *Lpin3*. Targeted 129/OlaHsd embryonic stem cells were injected into C57BL/6J blastocysts. Male chimeric mice were mated with C57BL/6J females, and the progeny were backcrossed to C57BL/6J mice. Wild-type and mutant alleles were detected by PCR with the following primer pairs: wild-type, tagagttgcctggactgtgg and tctggtgttggcttttcc; mutant, ttatcgatgagcgtggtggtt and gcgcgtacatcgggcaaataa. Animals heterozygous for the *fld* allele (a nonfunctional *Lpin1* allele that arose by spontaneous mutation [14]) were obtained from The Jackson Laboratory (Bar Harbor, ME). The *fld* mice were mated with $Lpin3^{+/-}$ mice, and the resulting $Lpin1^{+/-}Lpin3^{+/-}$ mice were intercrossed to obtain $Lpin1^{-/-}Lpin3^{-/-}$ (*Lpin1/3*KO) mice as well as wild-type and single-knockout littermates.

All mice were housed under 12-h light–dark conditions and fed a chow diet containing 4.5% fat and 50% carbohydrate by weight (Lab Diet 5001, Purina, St. Louis, MO). In specified studies, mice were fed a high-fat diet containing 35% fat and 33% carbohydrate (Diet F3282, Bio-Serv, Frenchtown, NJ). Animal studies were approved by UCLA's Animal Research Committee.

2.2. Adipocyte differentiation studies

Mouse 3T3-L1 cells were obtained from Zen-Bio (Research Triangle Park, NC) and grown to confluency in a preadipocyte medium containing DMEM with bovine calf serum (Zen-Bio #PM-1-L1). 48 h post-confluence (day 0), cells were induced to differentiate with an adipogenic medium containing dexamethasone, insulin, isobutylmethylxanthine, a PPARγ agonist, and FBS (Zen-Bio #DM-2-L1). After 3 days, the cells were switched to an adipocyte maintenance medium containing insulin, dexamethasone, and FBS (Zen-Bio #AM-1-L1), and the medium was refreshed every other day. Cells were collected in RiboZol reagent (Amresco, Solon, OH) on days 0, 3, 6, 10, and 14, and total RNA was isolated.

Human subcutaneous primary preadipocytes from middle-aged female donors with a normal body mass index (mean, 26.8 kg/m^2) were obtained from Zen-Bio and differentiated with an adipogenic medium containing dexamethasone, insulin, isobutylmethylxanthine, a PPARγ agonist, and FBS (Zen-Bio #DM-2). After 7 days, the cells were placed in an adipocyte maintenance medium containing insulin, dexamethasone, and FBS (Zen-Bio #AM-1). Cells were collected in RiboZol on days 0, 4, 8, and 14.

Mouse stromal vascular cells were isolated from inguinal fat pads of wild-type and *Lpin3*KO mice. The tissue was minced and incubated for 1 h with shaking at 37 °C in 3 ml of HEPES:collagenase solution (0.1 M HEPES, 0.12 M NaCl, 50 mM KCl, 5 mM D-glucose, 1.5% BSA, 1 mM $CaCl_2$, and 1000 units/ml collagenase). Samples were centrifuged at 50 × *g* for 5 min. The upper layer of tissue debris was discarded and the middle layer was centrifuged again at 200 × *g* for 10 min to pellet the stromal vascular cells, which were plated in DMEM containing 10% FBS. 48 h post-confluence (day 0), cells were induced to differentiate in 1 μM dexamethasone, 5 μg/ml insulin, 0.5 mM isobutylmethylxanthine, 1 μM rosiglitazone, and 10% FBS. After 2 days, the cells were maintained with insulin, rosiglitazone, and FBS, and the medium was refreshed every other day. On day 6, cells were collected in RiboZol reagent for RNA isolation, or fixed with 10% formalin for 1 h and stained with Oil Red O in 60% isopropanol.

2.3. Lipin-1 and lipin-3 subcellular localization

COS-7 cells were transfected with lipin-1-V5 or lipin-3-myc in pcDNA3.1, separately or in combination. After 48 h, cells were fixed with 4% paraformaldehyde, permeabilized with 0.2% saponin, and incubated with primary antibodies (mouse anti-V5 for lipin-1 or rabbit anti-myc for lipin-3) at a dilution of 1:500. After washing, the cells were incubated with fluorescent-labeled secondary antibodies [donkey anti-mouse Cy3 (red) or donkey anti-rabbit Alexa Fluor 488 (green)]. Nuclei were counterstained with DAPI, and the cells were visualized by confocal microscopy.

2.4. Biochemical and molecular analyses.

For gene expression analyses, cells were collected or tissues were homogenized in RiboZol reagent and processed to isolate total RNA, which was reverse-transcribed into cDNA with the iSCRIPT kit (Bio-Rad, Hercules, CA). Real-time quantitative PCR (qPCR) was performed on a Bio-Rad iCycler with the SsoFast EvaGreen Supermix reagent and protocol (Bio-Rad). Plate setup and analysis were performed as described [24].

Western blot analyses were performed as previously described [7,22], with minor modifications. Tissues were homogenized or cells were lysed in lysis buffer [250 mM sucrose, 20 mM Tris, 1 mM EDTA, 1.4% Triton X-100, 1 × Complete Mini EDTA-free protease inhibitor cocktail (Roche Diagnostics GmbH, Mannheim, Germany), 1 × phosphatase inhibitor cocktail 1, and 1 × phosphatase inhibitor cocktail 2 (Sigma, St. Louis, MO)] and centrifuged to remove debris. Protein lysates (40 μg for liver, 80 μg for adipose tissue, 20 μg for cultured cells) were run on a 3–8% Tris-acetate gel, transferred to nitrocellulose membrane, and blotted with primary antibody, followed by HRP-conjugated secondary antibody and detection by chemiluminescence (ECL2 kit #80196, Thermo Fisher, Rockford, IL). The lipin-1 antibody was a gift of Dr. Maroun Bou Kahlil (University of Ottawa, Ottowa, Ontario). The lipin-2 antibody was a gift of Dr. Brian Finck (Washington University, St. Louis, MO). The lipin-3 antibody was from Lifespan Biosciences (#C37207, Seattle, WA). The β-actin antibody was from Sigma (#A1978, St. Louis, MO).

PAP activity was measured in tissue lysates as described [4,16]. Briefly, fresh tissue was homogenized in PAP lysis buffer [250 mM sucrose, 2 mM dithiothreitol, 0.15% Tween-20, phosphatase inhibitor cocktails 2 and 3 (Sigma, St. Louis), 1 × Complete Mini EDTA-free protease inhibitor cocktail (Roche Diagnostics GmbH, Mannheim, Germany)], flash-frozen, and stored at −80 °C. PAP activity was measured at pH 6.5 and 37 °C with liposomes containing a 0.6 mM [^{3}H]PA substrate (made from [^{3}H]palmitate) with 0.4 mM phosphatidylcholine in 100 mM tris/maleate buffer with 5 mM $MgCl_2$, 2 mg/ml fatty acid-poor BSA, and 0.05% Tween-20. The reaction was halted with chloroform containing 0.08% olive oil as an acylglycerol carrier, and basic alumina was added to remove any PA or [^{3}H]palmitate formed by phospholipase A activity. The [^{3}H]DAG product was quantified by scintillation counting. Starting lysate amounts and incubation times were optimized to achieve < 15% PA consumption, and three different protein concentrations per sample were analyzed to ensure linearity of the assay. Parallel assays were performed in the

presence of the inhibitor NEM (5 mM) to assess the contribution of PAP-2 activity, which was then subtracted to obtain lipin PAP activity levels.

Triacylglycerol concentration in tissue extracts was determined with a colorimetric biochemical assay (L-Type triglyceride M, Wako, Richmond, VA) and normalized to total protein concentration.

2.5. Metabolic characterization

Mice were fasted for 5 h (0800–1300) before blood and tissue collection. Blood glucose was measured with a OneTouch Ultra Blood Glucose monitor (LifeScan, Milpitas, CA). Plasma lipid levels (triglycerides, free fatty acids, total cholesterol, HDL cholesterol, and unesterified cholesterol) were determined as described [25]. Plasma chemistries (alanine aminotransferase, aspartate aminotransferase, total bilirubin, albumin, γ-glutamyl transpeptidase, blood urea nitrogen, inorganic phosphorus, creatine kinase, cholesterol, total protein, glucose, and amylase) were measured on an ACE Alera automated biochemistry analyzer (Alfa Wassermann, West Caldwell, NJ).

2.6. Correlation of gene expression with adiposity traits in the Hybrid Mouse Diversity Panel (HMDP)

The HMDP strains, phenotypic analyses, and gene-expression profiling have been described previously [26,27]. Briefly, 114 inbred and recombinant inbred mouse strains (4–6 mice/strain) were assessed at 16 weeks of age for body composition with an EchoMRI instrument. Individual fat pats were dissected and weighed, and adipose tissue gene expression was evaluated with Affymetrix microarrays (Mouse Genome HT_MG430A arrays, Santa Clara, CA). We then tested correlations of *Lpin1*, *Lpin2*, *Lpin3*, and *Pparg* expression. The adiposity traits were highly correlated with one another and therefore cannot be considered independent.

2.7. Statistics

For pairwise comparisons, a Student's *t*-test was used. For comparisons involving multiple genotypes, two-way ANOVA was used, with *Lpin1* genotype (WT or KO) and *Lpin3* genotype (WT or KO) as the two covariates. For the growth curves (Figures 4D and S4B), linear regression was performed separately for male and female mice, with

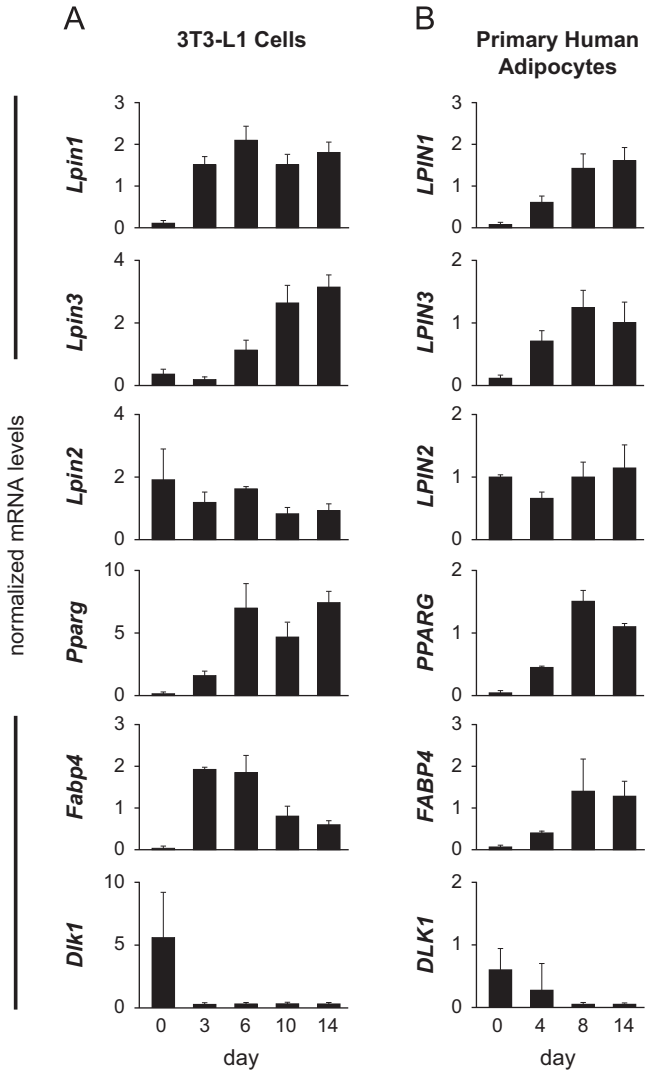

Figure 1: Lipin-3 is regulated during adipogenesis. qPCR analysis of gene expression during adipogenesis of (A) the mouse 3T3-L1 preadipocyte cell line and (B) human primary preadipocytes from day 0 to day 14 after induction by adipogenic cocktail. $n=3$ wells/time point.

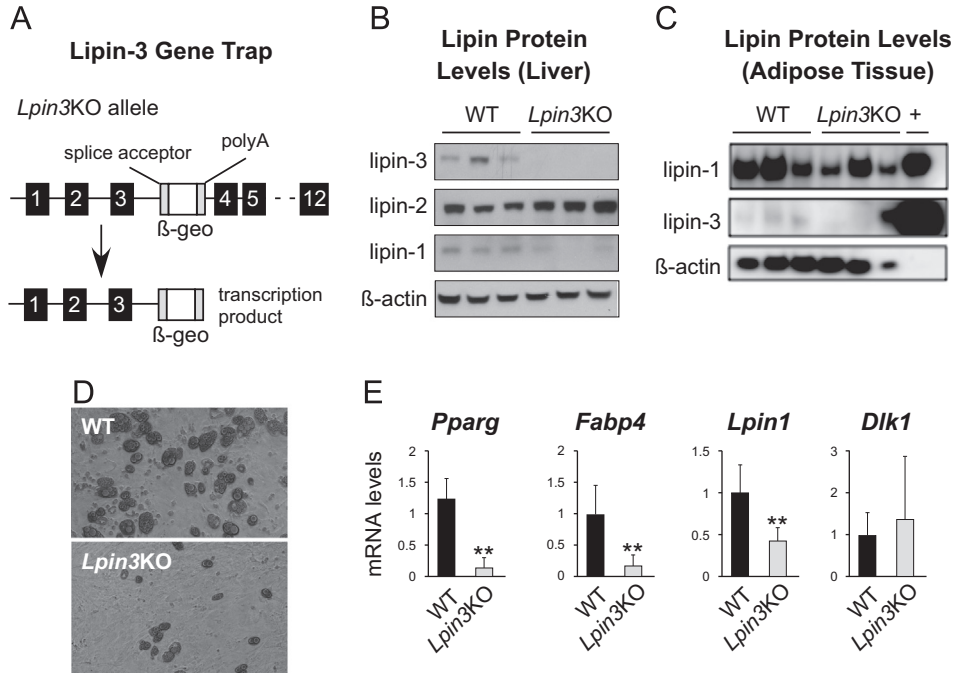

Figure 2: *Lpin3*KO stromal vascular cells exhibit impaired adipogenesis. (A) Generation of *Lpin3*KO mice. A β-geo element preceded by a splice acceptor was placed between exons 3 and 4 of *Lpin3*. Resulting transcripts contain *Lpin3* exons 1–3 spliced to β-geo, causing a truncated fusion protein that lacks PAP activity and other known lipin functional elements. (B, C) Western blot analysis of lipin protein levels in liver and adipose tissue from WT and *Lpin3*KO mice; $n=3$ per genotype. β-actin serves as a loading control. (D) Impaired lipid accumulation (dark droplets) 6 days after differentiation induction in stromal vascular cells isolated from *Lpin3*KO mice. Images are representative of independent experiments with 6 wild-type (WT) and 7 *Lpin3*KO mice (see also Figure S3). Bright field images at 200 × magnification. (E) qPCR analysis of gene expression at 6 days after differentiation induction. $n=6–7$ biological replicates/genotype; $^{**}p < 0.01$ compared to WT.

age, *Lpin1* genotype, and *Lpin3* genotype as the three covariates. For all comparisons, an alpha value of 0.05 was used.

3. RESULTS

3.1. Lipin-3 is regulated during mouse and human adipogenesis

Lpin1 expression is highly induced during adipocyte differentiation [28] (Figure 1A). Analysis of 3T3-L1 murine preadipocytes and primary human preadipocytes revealed that *Lpin3* and *LPIN3* expression are also induced during adipogenesis (~8-fold), whereas *Lpin2*/*LPIN2* expression is not regulated (Figure 1A and B). As expected, *Pparg/PPARG* and *Fabp4/FABP4* expression levels increased during adipocyte maturation, while *Dlk1/DLK1* expression fell (Figure 1A and B). These results led us to hypothesize that both lipin-1 and lipin-3 play a role in adipocytes.

3.2. Lipin-3-deficient mice exhibit subtle metabolic abnormalities

To assess the relevance of lipin-3 in adipogenesis, we created lipin-3 knockout (*Lpin3*KO) mice by introducing a promoterless β-geo cassette (a fusion of β-galactosidase and neomycin resistance genes) into intron 3 of *Lpin3* (Figure 2A). The mutant allele expresses a transcript containing sequences from the first three exons of *Lpin3* fused to β-geo; the predicted protein product lacks the majority of lipin-3 protein sequence, including the PAP and coactivator motifs. Lipin-3 deficiency was confirmed by analyzing mRNA and protein levels (Figure 2B and C). *Lpin3*KO mice were born at the expected Mendelian frequency, and their gross appearance was indistinguishable from wild-type mice. In both mice and humans, lipin-3 mRNA is expressed in metabolic tissues (*e.g.*, small intestine, kidney, liver, adipose tissue) [4], and we therefore assessed body and tissue weights, body composition, and plasma lipid levels in *Lpin3*KO mice. Lipin-3 deficiency did not affect body weight or tissue weight on a chow diet (Figures S1A and S2A and B), nor did it affect weight gain on a high-fat diet (Figure S1B). At an advanced age (14–16 months), *Lpin3*KO mice had slightly reduced body weight, but tissue weights and plasma lipid levels were within the normal range (Figures S1C and S2C).

3.3. Lipin-3 deficiency impairs the adipogenic potential of stromal vascular cells

Although *Lpin3*KO mice did not exhibit an overt metabolic phenotype, the striking induction of lipin-3 expression during mouse and human adipocyte differentiation suggested a local role in adipose tissue. We therefore tested whether lipin-3 deficiency affects adipogenesis in stromal vascular cells from fat pads of wild-type and *Lpin3*KO mice. Lipin-3 deficiency led to a reduced capacity for adipocyte development. Compared with the wild-type cells, a smaller proportion of lipin-3-deficient cells accumulated lipid droplets, and the droplets were smaller (Figures 2D and S3). Furthermore, the expression of genes that promote adipogenesis (*e.g.*, *Pparg*, *Fabp4*, *Lpin1*) was attenuated in *Lpin3*KO adipocytes. *Dlk1* expression levels after 6 days of differentiation were very low and were similar in wild-type and KO cells (Figure 2E).

3.4. Combined presence of lipin-1 and lipin-3 influences lipin subcellular localization and protein levels

Primary preadipocytes from lipin-1-deficient [24] and lipin-3-deficient mice (Figure 2D and E) each exhibit impaired adipocyte differentiation *in vitro*. Given the precedence for lipin-1 and lipin-2 protein cooperation in tissues such as brain and liver [22], we hypothesized that lipin-1 and lipin-3 may also function together. In support of this

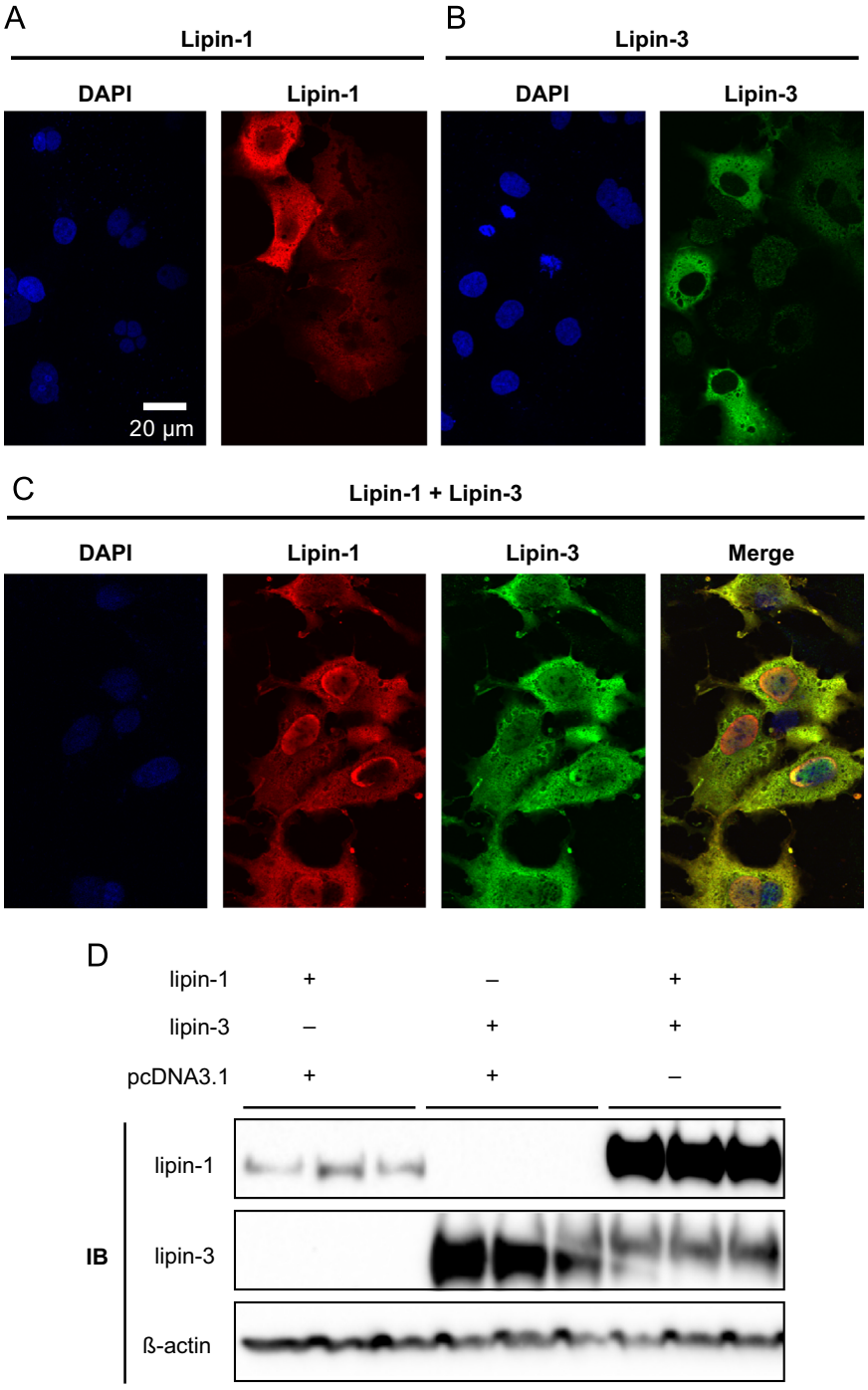

Figure 3: Lipin-1 and lipin-3 influence the subcellular localization and levels of one another. (A–C) Representative confocal microscopy analysis of COS-7 cells transfected with lipin-1-V5 plasmid (A), lipin-3-myc plasmid (B), or both plasmids (C). The cells were then visualized by confocal immunofluorescence microscopy with anti-V5 or anti-myc primary antibodies, followed by secondary antibodies labeled with Cy3 (red) or Alexa Fluor 488 (green). (D) HEK 293T cells were transfected with plasmids for lipin-1-V5 and lipin-3-myc independently or in combination. Plasmid quantity was kept constant with the addition of empty vector (pCDNA3.1), as indicated. After 48 h, cells were collected and proteins analyzed by Western blot.

possibility, we observed that the co-expression of lipin-1 and lipin-3 in cultured cells influences the subcellular localization and the levels of the two lipins. When expressed alone in HEK 293 cells, lipin-1 localized primarily to the cytoplasm, with low amounts in the nucleus (Figure 3A). Lipin-3 expressed alone localized exclusively to the cytoplasm (Figure 3B). When lipin-1 and lipin-3 were expressed together, the localization of both lipins was altered. The cytoplasmic localization of lipin-1 was reduced, and a significant amount of the lipin-1 was concentrated in the perinuclear region; lipin-3 was visible in both the nucleus and the cytoplasm (Figure 3C). Also, we observed substantial co-localization of lipin-1 and lipin-3 in the cytoplasm, the perinuclear region, and the nucleus (Figure 3C, yellow areas in the merged image).

The combined presence of lipin-1 and lipin-3 also influenced lipin protein levels. Co-expression of lipin-1 and lipin-3 from a heterologous promoter led to dramatically increased lipin-1 protein levels compared to

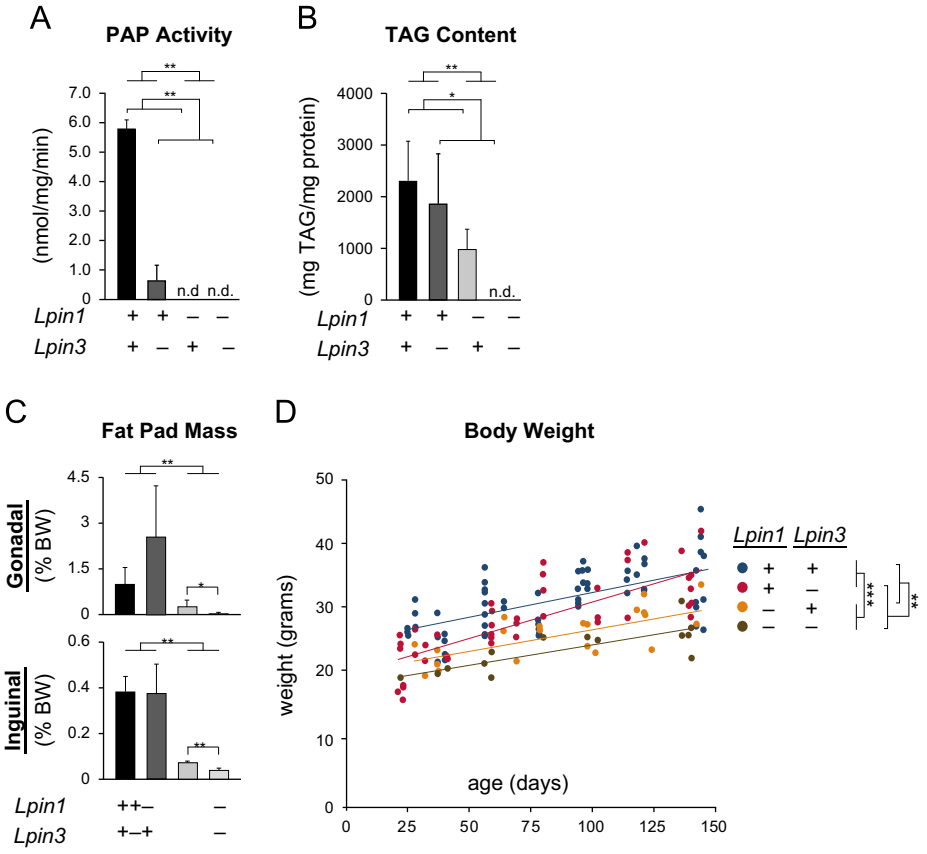

Figure 4: Lipin-3 is critical for optimal PAP activity in adipose tissue and a determinant of adiposity *in vivo*. PAP activity levels (A) and triacylglycerol (TAG) content (B) of adipose tissue from WT, *Lpin1*KO, *Lpin3*KO and *Lpin1/3*KO mice. Values represent mean ± SD from 4 mice per genotype, analyzed at 1 month of age; n.d., not detectable. (C) Lipin-3 deficiency exacerbates lipodystrophy in *Lpin1*KO mice. Gonadal and inguinal (subcutaneous femoral) fat depot size expressed as percent body weight at 6 months of age for indicated genotypes; $n = 4$–6/genotype. (D) Body weight as a function of age, separated by genotype. Dots represent independent data points and lines represent best-fit regression lines. Groups with statistically significant differences are indicated by brackets in figure legend; $n = 146$ male mice. For (A–D), $^{*}p < 0.05$; $^{**}p < 0.01$; $^{***}p < 0.001$.

Trait	Correlation coefficients			
	Lpin1	*Lpin3*	*Lpin2*	*Pparg*
Femoral fat pad, raw	−0.465****	−0.398****	n.s.	−0.312**
(As % body weight)	−0.524****	−0.401****	n.s.	−0.331**
Mesenteric fat pad, raw	−0.381***	−0.272**	n.s.	−0.270**
(As % body weight)	−0.360***	−0.284**	n.s.	−0.269**
Gonadal fat pad, raw	−0.468****	−0.263*	n.s.	−0.330**
(As % body weight)	−0.461****	−0.223*	n.s.	−0.318**
Retroperitoneal fat pad, raw	−0.379****	−0.243*	n.s.	−0.279**
(As % body weight)	−0.402***	−0.239*	n.s.	−0.268**
Total body fat, raw	−0.448****	−0.322**	n.s.	−0.309***
(As % body weight)	−0.522****	−0.331**	n.s.	−0.354**
Glucose-to-insulin ratio	0.270**	0.294**	n.s.	n.s.

Table 1: *Lpin1* and *Lpin3* expression levels are correlated with adiposity in mice. Statistically significant correlation coefficients between gene expression and adiposity or metabolic traits are listed. $^{*}p < 0.05$. $^{**}p < 0.01$. $^{***}p < 0.001$. $^{****}p < 0.0001$. n.s., not significant.

expression of the same amount of lipin-1 plasmid alone; expression of lipin-1 in combination with lipin-3 led to modestly reduced lipin-3 levels (Figure 3D). Taken together, these *in vitro* studies revealed a complex relationship between lipin-1 and lipin-3, and provided impetus to examine the roles of lipin-1 and lipin-3 *in vivo*.

3.5. Lipin-3 is required for optimal PAP activity in adipose tissue

Our *in vitro* studies indicated roles for both lipin-1 and lipin-3 in adipocytes, but the lack of an overt adipose tissue phenotype in *Lpin3*KO mice suggested at least partial compensation by lipin-1 *in vivo*. To clarify the roles of lipin-1 and lipin-3 *in vivo*, we analyzed adipose tissue in mouse models expressing both proteins, each protein independently, or neither protein. We crossed lipin-1-deficient *Lpin1*$^{fld/fld}$ mice (referred to as *Lpin1*KO mice) with *Lpin3*KO mice to yield four groups of mice: wild-type (WT), *Lpin1*KO, *Lpin3*KO, and *Lpin1/3*KO. To identify unique and cooperative roles for lipin-1 and lipin-3, we assessed the effects of lipin-1 and lipin-3 activity across all four groups with two-way ANOVA, using *Lpin1* genotype (WT or KO) and *Lpin3* genotype (WT or KO) as the two covariates.

We first assessed the effects of lipin-1 and lipin-3 deficiencies on PAP activity and TAG content in adipose tissue (Figure 4A and B). In agreement with earlier studies [3,4], lipin-1 was critical for adipose tissue PAP activity. To our surprise, lipin-3 deficiency also had a profound effect on adipose tissue PAP activity, reducing it by 85% (0.66 ± 0.5 nmol/mg/min *vs.* 5.8 ± 0.4 nmol/mg/min in wild-type mice). Despite the reduced adipose tissue PAP activity, the adipose tissue in the single-knockout mice retained 40–80% of wild-type TAG levels. In contrast, the loss of both lipin-1 and lipin-3 led to undetectable TAG within adipose tissue (Figure 4B).

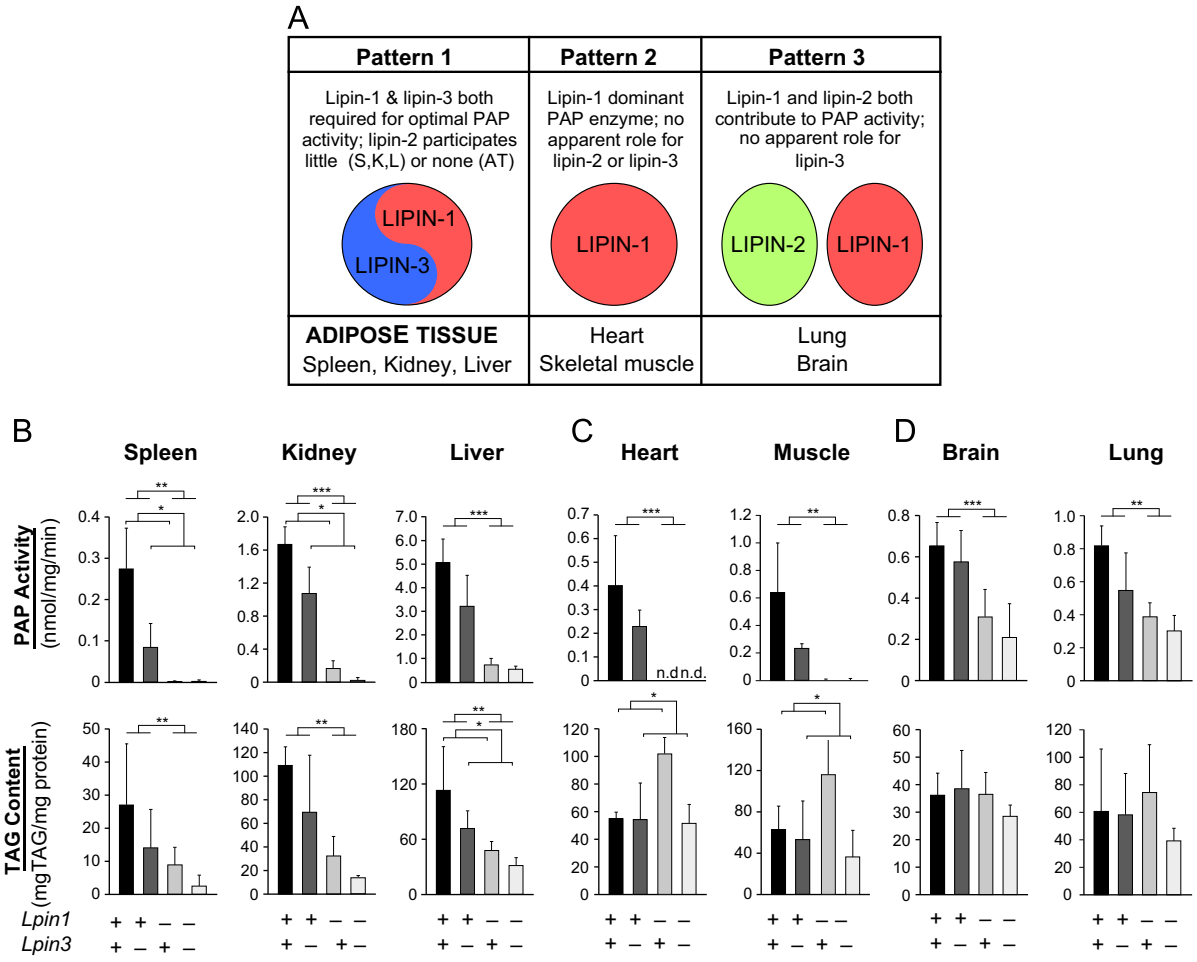

Figure 5: Contribution of lipin-1, lipin-2, and lipin-3 to PAP activity in metabolic tissues. (A) PAP activity was measured in 7 non-adipose tissues of WT, *Lpin1*KO, *Lpin3*KO and *Lpin1/3*KO mice. Three patterns were observed. Pattern 1 is defined by a requirement for both lipin-1 and lipin-3, such that loss of either protein results in a dramatic loss of PAP activity, suggesting a cooperative relationship between lipin-1 and lipin-3. In addition to adipose tissue, this pattern was observed in spleen, kidney, and liver (B). Pattern 2 was observed in heart and skeletal muscle, where the only determinant of PAP activity was lipin-1 (C). Pattern 3 was observed in lung and brain, where lipin-1 and lipin-2 contributed additively to PAP activity (D).

3.6. Lipin-1 and lipin-3 together influence adiposity *in vivo*

Consistent with the roles for both lipin-1 and lipin-3 in adipose tissue PAP activity, both lipin-1 and lipin-3 influenced adiposity *in vivo*. As expected, fat pad size in lipin-1-deficient mice was markedly lower than in wild-type mice (Figures 4C and S4A). Lipin-3 deficiency alone did not affect fat pad mass, but fat pad sizes in *Lpin1/3*KO mice were smaller than in *Lpin1*KO mice (Figures 4C and S4A).

The effect of lipin-1/3 deficiency on fat pad mass was reflected in total body weight. We measured body weight in 303 mice (146 males, 157 females) and performed linear regression with age, *Lpin1* genotype, and *Lpin3* genotype as independent predictors of body weight. Males and females were analyzed separately. As expected, *Lpin1*KO mice were significantly smaller than wild-type littermates, both for males ($p < 0.001$) and females ($p < 0.001$) (Figures 4D and S4B). In males, lipin-3 deficiency also lowered body weight ($p < 0.01$) (Figure 4D). Females exhibited the same trend (Figure S4B). Thus, lipin-1 and lipin-3 are independent determinants of body weight.

The effects of lipin-1/3 deficiency on body weight were largely due to effects in adipose tissue, given that liver, kidney, heart, and spleen weights were similar in the four groups of mice (except for a slightly larger kidney size in lipin-1-deficient mice at 12 months of age) (Figure S5). Plasma chemistry measurements, including markers of kidney, liver, muscle, and pancreas function, revealed no abnormalities associated with lipin-1 or lipin-3 deficiency (Figure S6).

3.7. Natural genetic variation in *Lpin3* expression is associated with adiposity

To determine whether naturally occurring genetic variations affecting *Lpin3* expression levels are associated with variations in adiposity *in vivo*, we took advantage of the Hybrid Mouse Diversity Panel [26,27]. This panel is a collection of 114 inbred and recombinant inbred mouse strains that have been characterized for metabolic traits and gene expression in adipose tissue. *Lpin1* expression levels in adipose tissue correlated with all adiposity traits measured: total body fat composition and weights of femoral, gonadal, retroperitoneal, and mesenteric fat depots (Table 1). This was true when expressed as absolute fat pad mass or as percent of body mass. *Lpin3* expression levels also correlated with these adiposity traits. Notably, the correlation coefficients for adiposity traits and *Lpin1*/*Lpin3* were of a similar magnitude as the correlation coefficient between adiposity traits and the expression of *Pparg*, a master regulator of adipogenesis (Table 1). *Lpin2* expression levels were not correlated with any of the adiposity traits. Finally, both *Lpin1* and *Lpin3*, but not *Pparg*, expression levels correlated with the fasting glucose-to-insulin ratio (Table 1).

3.8. Contribution of three lipin family members to PAP activity across metabolic tissues

The *Lpin1/3*KO mouse cohort provided a unique model in which to assess the contributions of lipin-1, lipin-2, and lipin-3 to PAP activity in metabolic tissues. As illustrated in Figure 4 for adipose tissue, the independent and cooperative effects of lipin-1 and lipin-3 are each evident by comparing the single and double knockout models. In addition, the contribution of lipin-2 can be inferred from PAP activity that remains in mice lacking both lipin-1 and lipin-3. The analysis of seven additional tissues from the *Lpin1/3*KO mouse cohort revealed three patterns of PAP activity (summarized in Figure 5A). Like adipose tissue, the spleen, kidney, and liver were dependent on both lipin-1 and lipin-3 for maximal PAP activity and TAG accumulation (Figure 5A and B). The milder effects of lipin-3 deficiency in spleen, kidney, and liver, compared with adipose tissue, may be due to prominent lipin-2 expression in those tissues [22].

A second PAP activity pattern, which was distinct from adipose tissue, occurred in heart and skeletal muscle (Figure 5A and C). In those tissues, lipin-3 was not critical for optimal PAP activity or TAG stores. Lipin-1 was essential for PAP activity in skeletal muscle and heart but did not correlate with TAG content (Figure 5C), in agreement with earlier studies [9,16]. A third PAP activity pattern was apparent in the brain and lung, where a deficiency in lipin-1, but not lipin-3, modestly affected PAP activity (Figure 5A and D). In those tissues, lipin-1 and lipin-2 appear to be the major determinants of PAP activity.

4. DISCUSSION

Lipins are the primary source of PAP activity in mammalian glycerolipid biosynthesis, but the extent to which each of the three family members contributes to PAP activity, TAG storage, and lipid homeostasis in different tissues has been unclear. Most studies of lipin physiology have focused on the roles of individual lipin paralogs through loss-of-function or gain-of-function approaches in cultured cells or mouse tissues. However, recent evidence suggests that cooperation between lipin family members is required for optimal lipid homeostasis in various tissues [22]. Here, we demonstrate that, in adipose tissue, lipin-3 cooperates with lipin-1 to achieve optimal PAP activity, TAG accumulation, and adiposity—functions that were previously attributed to lipin-1 alone [4]. Our findings in adipose tissue contribute to the concept that lipin enzymes function in an interdependent manner to achieve lipid homeostasis *in vivo*.

At the outset of our study, we observed that lipin-3 is induced during mouse and human adipogenesis. We also showed that lipin-1 and lipin-3 protein levels and subcellular localization are influenced by one another in cultured cells. Lipin localization is thought to be a determinant of PAP and coactivator activities [6,10,29], and could potentially influence lipin protein turnover as well. Factors known to influence lipin protein localization—and presumably function—include phosphorylation state, sumoylation, and interaction with 14-3-3 proteins [3,30–32]. Direct interaction of lipin proteins could also influence localization and/or protein levels. Along these lines, Liu et al. [33] detected lipin-1 homodimers, as well as heterodimers with lipin-2 and lipin-3, in co-immunoprecipitation studies. The current findings suggest that lipin regulation depends, in part, on tissue-specific functional interactions between different lipin family members.

To evaluate the *in vivo* relevance of lipin-3 in adipose tissue, we created lipin-3-deficient mice. Stromal vascular cells isolated from *Lpin3*KO fat exhibited impaired adipogenesis, with reduced levels of adipogenic gene expression and reduced lipid accumulation, similar to findings with preadipocytes from *Lpin1*KO mice [24,34]. The impairment observed during adipocyte differentiation *ex vivo* was not apparent in adipose tissue from *Lpin3*KO mice, likely due to compensatory mechanisms that are active *in vivo*. Similar observations have been reported for other adipogenic genes, including those for adipocyte transcription factors C/EBPβ and C/EBPδ [35]. The *Lpin3*KO mice did, however, exhibit modestly reduced body weight with advanced age. We suspected that lipin-1 in *Lpin3*KO adipose tissue partially compensated for the loss of lipin-3.

To better define the functional relationship between lipin-1 and lipin-3 in adipose tissue, we generated *Lpin1/3*KO mice and compared them to wild-type, *Lpin1*KO, and *Lpin3*KO mice. Unexpectedly, adipose tissue PAP activity was reduced by more than 85% in the absence of *either* lipin-1 or lipin-3. This finding implied that lipin-1 and lipin-3 work cooperatively to achieve optimal PAP function, rather than each contributing to total PAP activity in an additive fashion. When both lipin-1 and lipin-3 were inactivated, adipose tissue PAP activity and TAG accumulation were abolished. Thus, lipin-1 and lipin-3—but not lipin-2—play a role in determining PAP activity in mouse adipose tissue.

*Lpin1/3*KO mice had more severely reduced fat pad mass, PAP activity, and TAG content than *Lpin1*KO mice, implying that the presence of lipin-3 compensates for the absence of lipin-1 in adipose tissue. These findings are intriguing and potentially relevant to lipin-1-deficient humans, where overt lipodystrophy is absent [19–21]. It seems likely that lipin-3 compensates for the loss of lipin-1 in human adipose tissue and thereby prevents clinically obvious lipodystrophy. We observed slight differences in the kinetics of lipin gene expression in cultured mouse and humans adipocytes: human *LPIN3* was induced very early during adipocyte differentiation—very much like *LPIN1*—whereas mouse *Lpin3* reached peak expression levels several days later than *Lpin1*. It is possible that lipin-2 also plays a role in adipocytes of mice and/or humans. Lipin-2 mRNA is expressed in human adipose tissue [4], as well as in mouse 3T3-L1 cells ([36] and this study). In their recent study in the mouse 3T3-L1 adipocyte cell line, Sembongi et al. demonstrated that lipin-2 protein is most prominent in stromal vascular cells of mouse adipose tissue, whereas lipin-1 is present in mature adipocytes [36]. Lipin-2 knockdown studies in 3T3-L1 cells led to increased lipid droplet volume, although total cellular TAG content did not change [36]. A role for lipin-2 in lipid droplet biogenesis or remodeling—rather than determining net TAG content—is consistent with our finding that lipin-2 does not influence adipose tissue TAG content or PAP activity *in vivo.* In contrast to our findings, Sembongi et al. [36] did not detect lipin-3 in mouse adipose tissue, and this could be related to numerous experimental differences (*e.g.*, amounts of protein, antibodies, and fat pad analyzed).

In addition to studies with knockout mice, we demonstrated that naturally occurring genetic variations in lipin-1 and lipin-3 expression levels are correlated with fat pad mass in several fat depots. These correlations were strongest for lipin-1, but lipin-3 correlations were of a similar magnitude to those observed for PPARγ, a key driver of adipogenesis. Interestingly, *Lpin1*, *Lpin3*, or *Pparg* expression levels were inversely correlated with adiposity, suggesting that feedback mechanisms may attenuate expression of these genes in mature mice when a sufficient level of adiposity is achieved. Studies in humans have also reported inverse relationships between lipin-1 levels and adiposity-related measurements including BMI, percent body fat, and the metabolic syndrome (reviewed in [29]).

The expression levels of *Lpin1* and *Lpin3* were correlated with glucose-to-insulin ratio. Because *Pparg* was not correlated with this trait, the influence of lipins on glucose and/or insulin pathways may be

independent of effects on adipose tissue development. Of note, a recent genome-wide association meta-analysis in humans uncovered a locus associated with fasting glucose levels for which *LPIN3* is a likely candidate [37].

In addition to the cooperation between lipin-1 and lipin-3 in adipose tissue, our survey of PAP activity across eight tissues revealed tissue-specific relationships between lipin family members. As summarized in Figure 5A, we detected three general patterns of lipin tissue activity in the mouse. In the first pattern, exemplified by adipose tissue, lipin-1 and lipin-3 act synergistically to achieve optimal PAP activity, while lipin-2 plays a negligible role. Variations on this pattern were observed in spleen, kidney, and liver, where some PAP activity is provided by lipin-2. In the second pattern, typified by heart and skeletal muscle, lipin-1 appears to be the major determinant of PAP activity, consistent with earlier reports [3,4,16]. In the third pattern, typified by lung and brain, lipin-1 and lipin-2 contribute to PAP activity in an additive fashion.

In summary, these studies add to a growing body of evidence that lipin protein function, and glycerolipid synthesis, are influenced by intricate functional interactions between lipin family members. Our results implicate lipin-3 as well as lipin-1 as a determinant of adiposity *in vivo*. This may have particular relevance in lipin-1-deficient humans, which lack overt lipodystrophy, perhaps due to lipin-3 activity in this tissue.

ACKNOWLEDGMENTS

We thank Jenny Link for advice concerning stromal vascular cell isolation and Dr. Peter Tontonoz for helpful discussions. We gratefully acknowledge support from the National Institutes of Health P01 HL090553 and P01 HL28481, and training grant T21HG002536.

CONFLICT OF INTEREST

The authors wish to confirm that there are no known conflicts of interest associated with this publication and there has been no significant financial support for this work that could have influenced its outcome.

APPENDIX A. SUPPORTING INFORMATION

Supplementary data associated with this article can be found in the online version at http://dx.doi.org/10.1016/j.molmet.2013.11.008.

REFERENCES

[1] Péterfy, M., Phan, J., Xu, P., Reue, K., 2001. Lipodystrophy in the *fld* mouse results from mutation of a new gene encoding a nuclear protein, lipin. Nature Genetics 27:121–124.

[2] Han, G.S., Wu, W.I., Carman, G.M., 2006. The *Saccharomyces cerevisiae* Lipin homolog is a Mg^{2+}-dependent phosphatidate phosphatase enzyme. Journal of Biological Chemistry 281:9210–9218.

[3] Harris, T.E., Huffman, T.A., Chi, A., Shabanowitz, J., Hunt, D.F., Kumar, A., et al., 2007. Insulin controls subcellular localization and multisite phosphorylation of the phosphatidic acid phosphatase, lipin 1. Journal of Biological Chemistry 282:277–286.

[4] Donkor, J., Sariahmetoglu, M., Dewald, J., Brindley, D.N., Reue, K., 2007. Three mammalian lipins act as phosphatidate phosphatases with distinct tissue expression patterns. Journal of Biological Chemistry 282:3450–3457.

[5] Csaki, L.S., Dwyer, J.R., Fong, L.G., Tontonoz, P., Young, S.G., Reue, K., 2013. Lipins, lipinopathies, and the modulation of cellular lipid storage and signaling. Progress in Lipid Research 52:305–316.

[6] Finck, B.N., Gropler, M.C., Chen, Z., Leone, T.C., Croce, M.A., Harris, T.E., et al., 2006. Lipin 1 is an inducible amplifier of the hepatic PGC-1alpha/PPARalpha regulatory pathway. Cell Metabolism 4:199–210.

[7] Donkor, J., Zhang, P., Wong, S., O'Loughlin, L., Dewald, J., Kok, B.P.C., et al., 2009. A conserved serine residue is required for the phosphatidate phosphatase activity but not the transcriptional coactivator functions of lipin-1 and lipin-2. Journal of Biological Chemistry 284:29968–29978.

[8] Kim, H.B., Kumar, A., Wang, L., Liu, G.H., Keller, S.R., Lawrence, J.C., et al., 2010. Lipin 1 represses NFATc4 transcriptional activity in adipocytes to inhibit secretion of inflammatory factors. Molecular and Cellular Biology 30:3126–3139.

[9] Mitra, M.S., Schilling, J.D., Wang, X., Jay, P.Y., Huss, J.M., Su, X., et al., 2011. Cardiac lipin 1 expression is regulated by the peroxisome proliferator activated receptor γ coactivator 1α/estrogen related receptor axis. Journal of Molecular and Cellular Cardiology 51:120–128.

[10] Harris, T.E., Finck, B.N., 2011. Dual function lipin proteins and glycerolipid metabolism. Trends in Endocrinology and Metabolism 22:226–233.

[11] Reue, K., Xu, P., Wang, X.P., Slavin, B.G., 2000. Adipose tissue deficiency, glucose intolerance, and increased atherosclerosis result from mutation in the mouse fatty liver dystrophy (*fld*) gene. Journal of Lipid Research 41:1067–1076.

[12] Xu, J., Lee, W.N.P., Phan, J., Saad, M.F., Reue, K., Kurland, I.J., 2006. Lipin deficiency impairs diurnal metabolic fuel switching. Diabetes 55:3429–3438.

[13] Langner, C.A., Birkenmeier, E.H., Roth, K.A., Bronson, R.T., Gordon, J.I., 1991. Characterization of the peripheral neuropathy in neonatal and adult mice that are homozygous for the fatty liver dystrophy (*fld*) mutation. Journal of Biological Chemistry 266:11955–11964.

[14] Langner, C.A., Birkenmeier, E.H., Ben-Zeev, O., Schotz, M.C., Sweet, H.O., Davisson, M.T., et al., 1989. The fatty liver dystrophy (*fld*) mutation. Journal of Biological Chemistry 264:7994–8003.

[15] Verheijen, M.H.G., Chrast, R., Burrola, P., Lemke, G., 2003. Local regulation of fat metabolism in peripheral nerves. Genes and Development 17:2450–2464.

[16] Kok, B.P.C., Kienesberger, P.C., Dyck, J.R.B., Brindley, D.N., 2012. Relationship of glucose and oleate metabolism to cardiac function in lipin-1 deficient (*fld*) mice. Journal of Lipid Research 53:105–118.

[17] Phan, J., Reue, K., 2005. Lipin, a lipodystrophy and obesity gene. Cell Metabolism 1:73–83.

[18] Donkor, J., Sparks, L.M., Xie, H., Smith, S.R., Reue, K., 2008. Adipose tissue lipin-1 expression is correlated with peroxisome proliferator-activated receptor alpha gene expression and insulin sensitivity in healthy young men. Journal of Clinical Endocrinology and Metabolism 93:233–239.

[19] Zeharia, A., Shaag, A., Houtkooper, R.H., Hindi, T., de Lonlay, P., Vaz, M., et al., 2008. Mutations in *LPIN1* cause recurrent acute myoglobinuria in childhood. American Journal of Human Genetics 83:489–494.

[20] Michot, C., Hubert, L., Brivet, M., De Meirleir, L., Valayannopoulos, V., Müller-Felber, W., et al., 2010. *LPIN1* gene mutations: a major cause of severe rhabdomyolysis in early childhood. Human Mutation 31:E1564–1573.

[21] Bergounioux, J., Brassier, A., Rambaud, C., Bustarret, O., Michot, C., Hubert, L., et al., 2012. Fatal rhabdomyolysis in 2 children with *LPIN1* mutations. Journal of Pediatrics 160:1052–1054.

[22] Dwyer, J.R., Donkor, J., Zhang, P., Csaki, L.S., Vergnes, L., Lee, J.M., et al., 2012. Mouse lipin-1 and lipin-2 cooperate to maintain glycerolipid homeostasis in liver and aging cerebellum. Proceedings of the National Academy of Sciences of the United States of America 109:E2486–2495.

[23] Friedel, R.H., Soriano, P., 2010. Gene trap mutagenesis in the mouse. Methods in Enzymology 477:243–269.

[24] Phan, J., Péterfy, M., Reue, K., 2004. Lipin expression preceding peroxisome proliferator-activated receptor-gamma is critical for adipogenesis *in vivo* and *in vitro*. Journal of Biological Chemistry 279:29558–29564.

[25] Barajas, B., Che, N., Yin, F., Rowshanrad, A., Orozco, L.D., Gong, K.W., et al., 2011. NF-E2-related factor 2 promotes atherosclerosis by effects on plasma lipoproteins and cholesterol transport that overshadow antioxidant protection. Arteriosclerosis, Thrombosis, and Vascular Biology 31:58–66.

[26] Bennett, B.J., Farber, C.R., Orozco, L., Kang, H.M., Ghazalpour, A., Siemers, N., et al., 2010. A high-resolution association mapping panel for the dissection of complex traits in mice. Genome Research 20:281–290.

[27] Ghazalpour, A., Rau, C.D., Farber, C.R., Bennett, B.J., Orozco, L.D., van Nas, A., et al., 2012. Hybrid mouse diversity panel: a panel of inbred mouse strains suitable for analysis of complex genetic traits. Mammalian Genome: Official Journal of the International Mammalian Genome Society 23:680–692.

[28] Zhang, P., O'Loughlin, L., Brindley, D.N., Reue, K., 2008. Regulation of lipin-1 gene expression by glucocorticoids during adipogenesis. Journal of Lipid Research 49:1519–1528.

[29] Csaki, L.S., Reue, K., 2010. Lipins: multifunctional lipid metabolism proteins. Annual Review of Nutrition 30:257–272.

[30] Péterfy, M., Harris, T.E., Fujita, N., Reue, K., 2010. Insulin-stimulated interaction with 14-3-3 promotes cytoplasmic localization of lipin-1 in adipocytes. Journal of Biological Chemistry 285:3857–3864.

[31] Liu, G.H., Gerace, L., 2009. Sumoylation regulates nuclear localization of lipin-1alpha in neuronal cells. PloS One 4:e7031.

[32] Peterson, T.R., Sengupta, S.S., Harris, T.E., Carmack, A.E., Kang, S.A., Balderas, E., et al., 2011. mTOR complex 1 regulates lipin 1 localization to control the SREBP pathway. Cell 146:408–420.

[33] Liu, G.H., Qu, J., Carmack, A.E., Kim, H.B., Chen, C., Ren, H., et al., 2010. Lipin proteins form homo- and hetero-oligomers. Biochemical Journal 432:65–76.

[34] Zhang, P., Takeuchi, K., Csaki, L.S., Reue, K., 2012. Lipin-1 phosphatidic phosphatase activity modulates phosphatidate levels to promote peroxisome proliferator-activated receptor γ (PPARγ) gene expression during adipogenesis. Journal of Biological Chemistry 287:3485–3494.

[35] Tanaka, T., Yoshida, N., Kishimoto, T., Akira, S., 1997. Defective adipocyte differentiation in mice lacking the C/EBPbeta and/or C/EBPdelta gene. EMBO Journal 16:7432–7443.

[36] Sembongi, H., Miranda, M., Han, G.-S., Fakas, S., Grimsey, N., Vendrell, J., Carman, G.M., Siniossoglou, S., 2013. Distinct roles fof the phosphatidate phosphatases lipin 1 and 2 during adipogenesis and lipid droplet biogenesis in 3T3-L1 cells. Journal of Biological Chemistry 288:34502–34513.

[37] Scott, R.A., Lagou, V., Welch, R.P., Wheeler, E., Montasser, M.E., Luan, J., et al., 2012. Large-scale association analyses identify new loci influencing glycemic traits and provide insight into the underlying biological pathways. Nature Genetics 44:991–1005.

